Sensors and Materials, Vol. 32, No. 1 (2020) 135–148
MYU Tokyo

S & M 2091

Application of Water Tank Employing Smart Sensor for Thermal–Electric Energy Conversion on Vehicles

Feng-Chia Chuang,[1†] Chun-Li Chang,[2] Yong-Neng Chow,[3]
Hui-Cun Shen,[1] Tung-Lung Wu,[1] Yi-Ching Chen,[4]
Chin-Sung Chiang,[4*] Fu-Lin Liao,[1] and Yi-Hui Chen[5]

[1]College of Mechanical and Automotive Engineering, Zhaoqing University,
Zhaoqing Avenue, Zhaoqing City, Guangdong Province 526061, China
[2]Yulin Normal University, Guangxi 537000, China
[3]School of Life Sciences, Zhaoqing University, Zhaoqing City, Guangdong Province 526061, China
[4]Department of Environmental Engineering, Da-Yeh University 51591, Taiwan
[5]Chaoyang Experimental School of Shantou City, Guangdong 515000, China

(Received August 20, 2019; accepted December 16, 2019)

Keywords: power generation, anti-theft water tank, thermoelectric power generation, recycling, vocational education

Generally, vehicles driven by fuels, such as gasoline, diesel, and aviation oil, are equipped with water tanks. These vehicles include vans, cars, heavy locomotives, fire engines, ambulances, aircraft, and boats. The cooling water in these water tanks absorbs the heat generated by engines and then gradually heats up. Nowadays, the heated cooling water is usually channeled into a radiator and returned to the water tank until the heat is dissipated. This has caused the problem of energy waste in the cold–hot conversion process, which increases the environmental impact of the vechicles. Therefore, in this research, a thermal power generation device is designed with a simple structure, composed of a Pt100 thermocouple thermometer and a thermistor with an LM358 operational amplifier as two different sensing devices. The designed device is expected to increase the power generation capacity without using additional energy for cooling thermoelectric power generation chips. Therefore, it is of great importance to cool the surface of the chips. Thermoelectric power generation chips are installed at the four corners of the front and rear of a water tank. The thermal energy generated by the water tank is used to generate electric energy, which achieves the purpose of energy recycling. The designed device is cost-effective and can achieve the purpose of reducing environmental impact and energy conservation. This research can be used as a reference for vocational education from the aspects of technology, management, design, technicalization, and research and development.

1. Introduction

To realize the recycling of thermal energy, the traditional heat-dissipating water tanks of heavy-duty locomotives are redesigned in this research. Specifically, a shield is mounted outside the water tank, and a detachable number plate is installed in the shield as a spare

*Corresponding author: e-mail: 778431798@qq.com
https://doi.org/10.18494/SAM.2020.2583

locomotive number to prevent the loss of the number plate due to theft or other reasons. At the same time, thermoelectric power generation chips are installed at the four corners of the front and rear panels of the shield to generate electric energy using the thermal energy generated by the water tank, thereby achieving energy recycling.

In this research, a thermal power generation device with a simple structure is designed. The device is expected to increase power generation capacity without using additional energy for cooling the thermoelectric power generation chips. Therefore, it is of great importance to cool the surface of the chips. During our experiment, a thermoelectric power generation chip, a flat panel heater, and a radiator with heat pipes and cooling fins are used to generate a temperature difference between the heater and the radiator. Then, electric energy is generated using the thermoelectric power generation chip. An actual situation where the designed thermal power generation device is applied is simulated. An anemometer and an infrared thermometer are also used to monitor the air flow rate around the cooling fins and the temperature of the experimental equipment.(1)

The heat generation effect is a phenomenon in which electrons/holes in a heated object move to generate current or accumulate electric charge due to a temperature gradient from a high-temperature region to a low-temperature region. Using a thermoelectric power generation chip, as shown in Fig. 1, thermal energy can be converted into electric energy using the temperature difference between the cold side and the hot side of the chip.(2)

The thermoelectric power generation module can generate electric energy via the temperature difference between the two ends of the module. In addition to large-scale thermoelectric systems, an energy hunting technology that collects small amount of energy is also a possible direction of future technological development. By collecting small amounts of energy in the environment, such a module can power portable electronic products, or be used in cases where wires cannot be used or batteries cannot be replaced conveniently. In this way, the

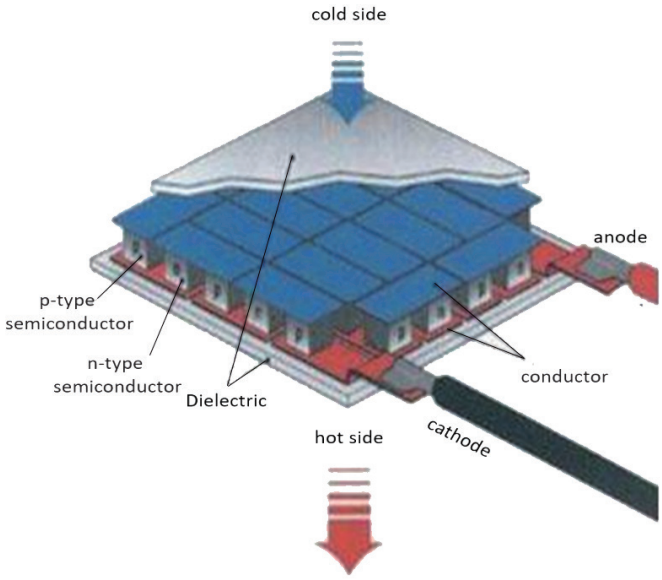

Fig. 1. (Color online) Thermoelectric power generation chip.

ambient temperature or human body temperature can be converted into electric energy using thermoelectric materials. Therefore, the thermoelectric power generation technology is of great significance for future energy reuse.[3]

2. Experimental

2.1 Thermoelectric effect

A thermoelectric material directly converts thermal energy into electric energy without the application of an external force, and the conversion process is reversible. Thermoelectric materials have three main effects, namely, the Seebeck effect and Peltier effect, as shown in Figs. 2 and 3, respectively, and the Thomson effect.[4]

2.2 Thermoelectric module principle and equivalent circuit

The thermoelectric module used in this research is based on the Seebeck effect; the upper part of the module is the hot side and the lower part is the cold side. In the case of a temperature difference, the majority of the carriers on the hot side of the P-type semiconductor will be moved toward the cold side, just like the current flowing from the hot side to the cold side. The majority of the carriers on the hot side of the N-type semiconductor will move from the hot side to the cold side, just like the flow of electrons from the hot side to the cold side, in the opposite direction to the current.[5,6]

As shown in Fig. 4, the temperature of the hot side is T_h, the temperature of the cold side is T_c, and the particle length and cross-sectional area of the semiconductor are L and A, respectively. For P-type thermoelectric particles, the Seebeck constant is α_p and the resistivity

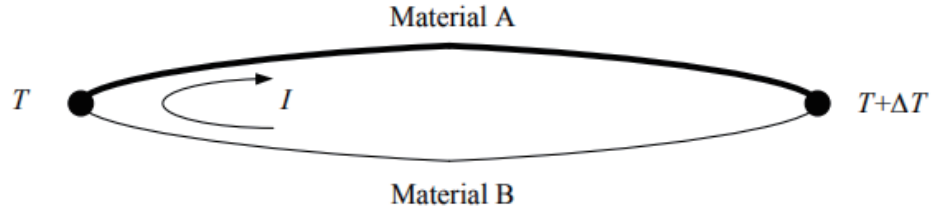

Fig. 2. Seebeck effect.

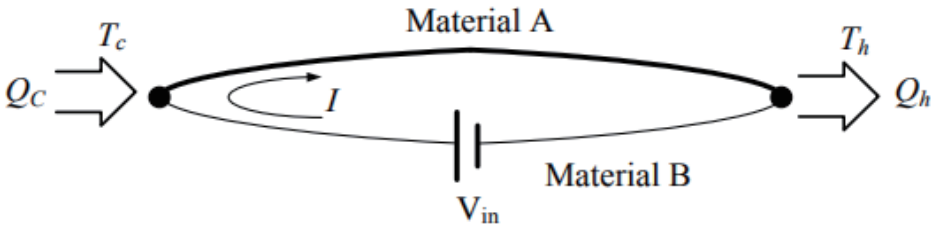

Fig. 3. Peltier effect.

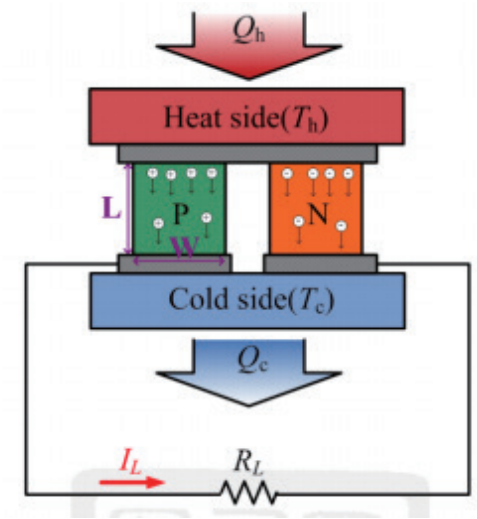

Fig. 4. (Color online) Overall diagram of the thermoelectric module and load.

is ρ_p; for N-type thermoelectric particles, the Seebeck constant is α_n and the resistivity is ρ_n. The generated open-circuit voltage V_s can be expressed as

$$V_s = \alpha(T_h - T_c)\,. \tag{1}$$

According to the resistance formula, the equivalent internal resistance R_s can be written as

$$R_s = (\rho_p - \rho_n)\frac{L}{A}\,. \tag{2}$$

The current generated is

$$I = \frac{V_s}{R_s + R_L} = \frac{(\alpha_p - \alpha_n)(T_h - T_c)}{R_s + R_L}\,. \tag{3}$$

The power obtained by the load is

$$P = \frac{\left[(\alpha_p - \alpha_n)(T_h - T_c)\right]^2}{(R_s + R_L)^2} R_L\,. \tag{4}$$

In the case of impedance matching, the maximum power obtained from the load is given by

$$P_{max} = \frac{\left[(\alpha_p - \alpha_n)(T_h - T_c)\right]^2}{4R_s} = \frac{V_s^2}{4R_s}\,. \tag{5}$$

From the aspect of heat conduction, the thermal energy flowing into the hot side and the cold side, respectively represented by Q_h and Q_n, can be written as

$$Q_h = (\alpha_p - \alpha_n) \times IT_h + (K_p + K_n)(T_h - T_c) - \frac{I^2 R_s}{2}, \tag{6}$$

$$Q_n = (\alpha_p - \alpha_n) \times IT_h + (K_p + K_n)(T_h - T_c) + \frac{I^2 R_s}{2}. \tag{7}$$

Equations (6) and (7) are composed of three parts, where $(\alpha_p - \alpha_n) \times IT_h$ represents the magnitude of the thermoelectric effect, $(I^2R_s)/2$ represents the Joule heat, and $(K_p + K_n)(T_h - T_c)$ is the Fourier effect. Equations (6) and (7) are the thermal conductance of P-type and N-type thermoelectric particles in the thermoelectric module, respectively. According to the conservation of energy, the difference between Eqs. (6) and (7) is the energy P produced by the thermoelectric module:

$$P = Q_h - Q_n = (\alpha_p - \alpha_n) \times (T_h - T_c) \times I - I^2 R_s. \tag{8}$$

The relationship between current and load R_L is

$$I = \frac{(\alpha_p - \alpha_n)(T_h - T_c)}{R_s + R_L}. \tag{9}$$

Substituting Eq. (8) into Eq. (9), we have

$$P = \frac{\left[(\alpha_p - \alpha_n)(T_h - T_c)\right]^2}{(R_s + R_L)^2} R_L = \frac{V_s^2}{(R_s + R_L)^2} R_L. \tag{10}$$

In addition, the power generation efficiency is defined as the ratio of the generated power to the thermal energy flowing into the hot side:

$$\eta = \frac{P}{Q_h}. \tag{11}$$

The maximum power generation efficiency is given by

$$\eta_{max} = \frac{P_{max}}{Q_h} = \frac{(T_h - T_c)}{T_h} \times \frac{\left[(1 + ZT_M)^{\frac{1}{2}} - 1\right]}{\left[(1 + ZT_M)^{\frac{1}{2}} - \frac{T_c}{T_h}\right]}, \tag{12}$$

where T_m is the average temperature of the hot and cold sides, and the thermoelectric figure of merit is defined as

$$Z = \frac{(\alpha_p - \alpha_n)^2}{(K_p + K_n)(R_p + R_n)}. \tag{13}$$

According to Eqs. (4) and (10), the same behavior of the thermoelectric module is obtained, and the correctness of the model is verified. It can be seen from the above equations that the thermoelectric power generation module includes the Seebeck voltage source V_s as a function of temperature and the equivalent internal resistance R_s, as shown in Fig. 5. The module is very similar to the equivalent model of the battery. Although Fig. 5 shows the actual equivalent model, it is usually used as the equivalent model of the thermoelectric module to simplify the construction of the built-in Seebeck electromotive force.[7]

Because the equivalent model of the thermoelectric module is equivalent to a DC voltage source connected in series with an equivalent resistance, the module is simular to a linear power supply. On the basis of the equivalent model of the thermoelectric module, the relationship between the output voltage and the output current is derived. Firstly, the relationship between its output voltage and current can be written as

$$I = \frac{V_s - V}{R_s}. \tag{14}$$

The output power can be written as

$$P = VI = \frac{V_s \times V - V^2}{R_s}. \tag{15}$$

Therefore, when V_s and R_s are known, the output characteristic curve can be drawn using Eqs. (14) and (15), as shown in Fig. 6. According to Eq. (1), increases in the temperature and open-circuit voltage will accordingly increase the Seebeck constant α.

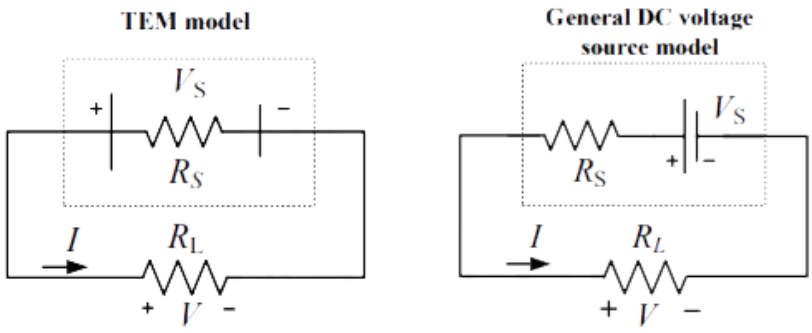

Fig. 5. Actual thermoelectric module and DC voltage source with internal resistance.

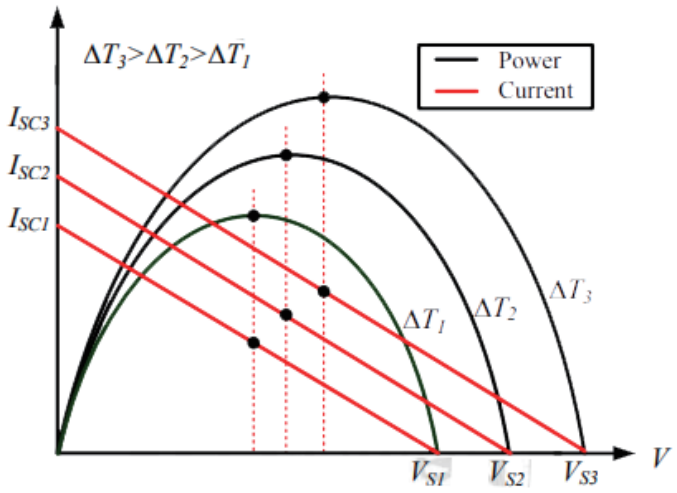

Fig. 6. (Color online) *P–V* and *I–V* output curves of the thermoelectric module.

According to the relationship between the output power and the output voltage shown in Eq. (14), the maximum power point is obtained when $\Delta P/\Delta V = 0$; thus, the differential result is expressed as

$$V = \frac{V_s}{2}. \tag{16}$$

It can be seen from Eq. (16) that when the impedance is matched, $R_L = R_s$, the operating voltage corresponding to the maximum power is half of the open-circuit voltage V_s. Many studies have developed maximum power tracking methods for thermoelectric modules using this characteristic of thermoelectric power modules. All these methods require periodic measurement of the open-circuit voltage V_s to ensure that the module is currently operating at the maximum power, but the measurement requires the thermoelectric power generation module to be disconnected from the back-end circuit. Thus, periodic measurement not only loses energy when measuring the open-circuit voltage, but also easily causes the instability of the system output. The power generation behavior of thermoelectric power generation modules has been extensively investigated in more detail. These studies on the modeling and analysis of thermoelectric modules have improved the effectiveness in predicting the expected power generation results when designing thermoelectric power generation systems.[8,9]

2.3 Thermoelectric power generation chip

A thermoelectric cooler, also called a refrigerating sheet or Peltier device, refers to a two-sided sheet, with one side absorbing heat and the other side dissipating heat. Such heat-conductive sheets do not generate cold themselves. The parameters of the thermoelectric cooler in this study are shown in Table 1.

Table 1
Parameters of the thermoelectric cooler.

Items	Front chip	Rear chip
External dimensions	40 × 3.63 mm^2	15 × 3.25 mm^2
Number of components	127	31
Internal resistance	2.3–2.5 Ω	0.85–1.0 Ω
Maximum temperature difference	65 °C	62 °C
Maximum working current	5.7 A	4.0
Nominal voltage	12 V	3.75 V
Refrigerating capacity	50 W	8–9 W
Work environment	−55–83 °C	−55–83 °C

2.4 Temperature feedback

A Pt100 platinum thermistor is used to feed back the tank temperature to a cellphone app in real time. The resistance of Pt100 is proportional to the temperature: when the temperature of Pt100 is 0 °C, its resistance is 100 Ω, and at 100 °C the resistance is about 138.5 Ω.

The circuit is designed to connect the three-wire Pt100 to the bridge and then amplify the signal through an LM358 operational amplifier to obtain a reference voltage value (i.e., the temperature corresponding to the current contact surface of Pt100). The circuit diagram and the resistance index table of Pt100 are shown in Fig. 7 and Table 2, respectively, where the circuit includes a Wheatstone bridge.

The resistance of Pt100 can be calculated by

$$R_t = R_0 \times (At + Bt^2 + c(t-100)^3), \tag{17}$$

where R_t is the resistance, R_0 is the resistance when Pt100 is at 0 °C, t is the temperature, $A = 3.940 \times 10^{-3}$, $B = -5.802 \times 10^{-7}$, and $C = -4.274 \times 10^{-12}$.[10]

Temperature conversion is achieved using the formula

$$V = 1024 \times \frac{R_t - 100}{1000} \times c, \tag{18}$$

where V is the AD input, R_t is the resistance connected in series with the thermal resistance in the bridge, c is the amplification factor of the operational amplifier, and the AD precision is $2^{10} = 1024$.

The magnification of the operational amplifier is given by

$$c = \left(1 + \frac{R7}{R4}\right) \times \left(1 + \frac{R9}{R8}\right) = \left(1 + \frac{10k}{10k}\right) \times \left(1 + \frac{10k}{10k}\right) = 4. \tag{19}$$

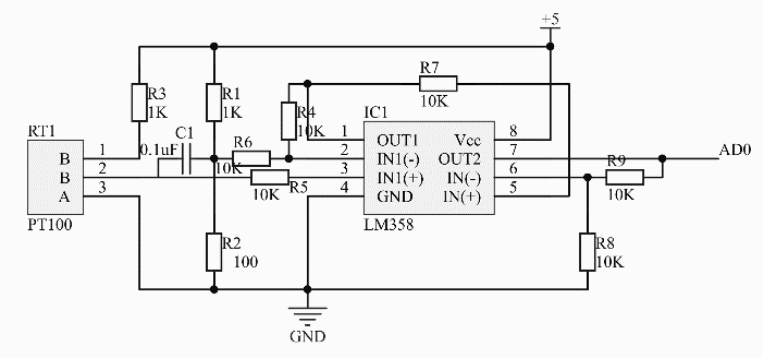

Fig. 7. Amplifying circuit with Wheatstone bridge.

Table 2
Resistance index table of Pt100.

℃	0	1	2	3	4	5	6	7	8	9
0	100	100.4	100.8	101.2	101.6	102	102.3	102.7	103.1	103.5
10	103.9	104.3	104.7	105.1	105.5	105.9	106.2	106.6	107	107.4
20	107.8	108.2	108.6	109	109.4	109.7	110.1	110.5	110.9	111.3
30	111.7	112.1	112.5	112.8	113.2	113.6	114	114.4	114.8	115.2
40	115.5	115.9	116.3	116.7	117.1	117.5	117.9	118.2	118.6	119
50	119.4	119.8	120.2	120.6	120.9	121.3	121.7	122.1	122.5	122.9
60	123.2	123.6	124	124.4	124.8	125.2	125.5	125.9	126.3	126.7
70	127.1	127.5	127.8	128.2	128.6	129	129.4	129.8	130.1	130.5
80	130.9	131.3	131.7	132	132.4	132.8	133.2	133.6	134	134.3
90	134.7	135.1	135.5	135.9	136.2	136.6	137	137.4	137.8	138.1
100	138.5	138.9	139.3	139.6	140	140.4	140.8	141.2	141.5	141.9
110	142.3	142.7	143.1	143.4	143.8	144.2	144.6	144.9	145.3	145.7
120	146.1	146.4	146.8	147.2	147.6	148	148.3	148.7	149.1	149.5
130	149.8	150.2	150.6	151	151.3	151.7	152.1	152.5	152.8	153.2
140	153.6	154	154.3	154.7	155.1	155.5	155.8	156.2	156.6	157
150	157.3	157.7	158.1	158.5	158.8	159.2	159.6	159.9	160.3	160.7
160	161.1	161.4	161.8	162.2	162.5	162.9	163.3	163.7	164	164.4
170	164.8	165.1	165.5	165.9	166.3	166.6	167	167.4	167.7	168.1
180	168.5	168.9	169.2	169.6	170	170.3	170.7	171.1	171.4	171.8
190	172.2	172.5	172.9	173.3	173.7	174	174.4	174.8	175.1	175.5
200	175.9	176.2	176.6	177	177.3	177.7	178.1	178.4	178.8	179.2

3. Results and Discussion

In accordance with the expected functions of the product, structure design and size calculation are preliminarily carried out, and then a manual drawing is performed in accordance with the design data. After that, CAD software is used for drawing, and the design results are shown in Figs. 8 and 9.

After the sketch design is completed, the three-dimensional modeling software UG is used for modeling. The front and rear panels of the shield are as shown in Figs. 10 and 11, respectively. The thermoelectric power generation chip is installed at the four corners of the panel, and a spare number plate is installed in the middle of the front panel. The vehicle's rear shield is shown in Fig. 11, and a motion simulation is performed on the vehicle model.

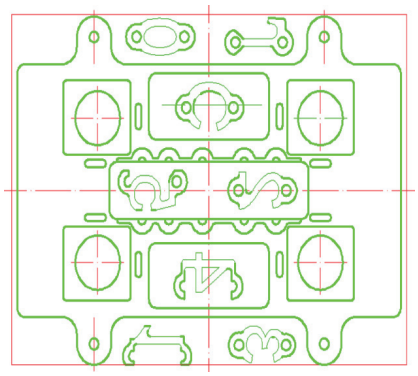

Fig. 8. (Color online) Design of front shield.

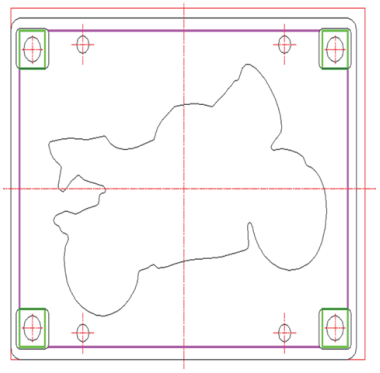

Fig. 9. (Color online) Design of rear shield.

Fig. 10. (Color online) Schematic of front shield.

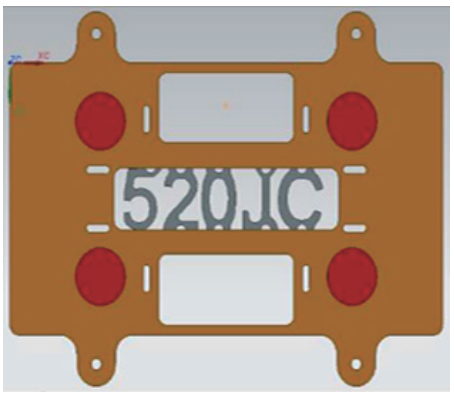

Fig. 11. (Color online) Schematic of rear shield.

The main alloying elements of 6061 aluminum alloy are magnesium and silicon, which form a Mg_2Si phase. If a certain amount of manganese or chromium is added to the alloy, the anti-fatigue and corrosion-resistance performances of the alloy can be improved. Sometimes a small amount of copper or zinc is added to increase the strength of the alloy without significantly reducing the corrosion-resistance performance. There is a small amount of copper in the conducting material to offset the adverse effects of titanium and iron on conductivity. Zirconium or titanium can refine grains and control the recrystallized structure. To improve the machinability, lead and antimony can be added. When Mg_2Si is solid-dissolved in aluminum, the alloy will possess an artificial age-hardening function. The 6061 aluminum alloy is an Al–Mg–Si alloy with medium strength, good plasticity, and excellent corrosion-resistance performance. In particular, the alloy does not tend to crack due to stress corrosion and also has excellent weldability and cold workability, making it a promising alloy with a wide range of applications.

The 6061 aluminum alloy can be anodized and colored, or painted with enamel, making it suitable for use as a building decoration material. It contains a small amount of Cu, giving it a higher strength alloy than 6063 aluminum alloy, but its quenching sensitivity is also higher than that of 6063 alloy. However, after compression, wind quenching cannot be achieved. Under

this condition, re-solution treatment and quenching aging are required to obtain higher strength. The mechanical and physical properties of the 6061 aluminum alloy are a yield strength of 5.51485 × 10^7 N/m^2, a tensile strength of 1.24084 × 10^8 N/m^2, an elastic modulus of 6.9 × 10^{10} N/m^2, a Poisson ratio of 0.33, a mass density of 2700 kg/m^3, a shear modulus of 2.6 × 10^{10} N/m^2, and a thermal expansion coefficient of 2.4 × 10^{-5} /K, as shown in Figs. 12 and 13.

Through the above static finite element analysis, it is found that the front shield is subjected to stress between 25.4982 and 19911.9 Pa, and its maximum stress is much smaller than the yield stress of 5.515 × 10^7 Pa. Also its displacement varies from 0 to 3.478902 × 10^{-5} mm, and the strain is in the range of 2.8742 × 10^{-10} – 2.04853 × 10^{-7}, which are both within the allowable range. Thus, the requirements for displacement and strain are met.

An analysis of the heat flow is conducted in the simulation module of SolidWorks software using the relationship between temperature changes and thermodynamic or physical parameters. The heat flow analysis can visualize the distribution and variation of heat on the shield, enabling the thermal energy to be more fully utilized. The heat flow analysis is performed on the front and rear panels. Using the engine as the heat source, the heat is transferred to the water tank. The water tank is fixed to the panel at a certain distance. The heat is generated by the engine and then transferred to the power generation chip through the water tank. Then electric energy is generated via the desired temperature difference. Considering the actual heat generation of the engine and the heat dissipation due to the wind, the temperature of the heat source is set at 60 °C.

The chip material is silicon with a thermal conductivity of 124 W/(mK) and a mass density of 2330 kg/m^3. The physical properties of the 40 × 40 chip are a mass of 0.0136445 kg, a volume of 5.85610^{-6} m^3, a density of 2330 kg/m^3, and a weight of 0.133716 N. The physical properties of the 15 × 15 chip are a mass of 0.00170906 kg, a volume of 7.335 × 10^{-7} m^3, a density of 2330 kg/m^3, and a weight of 0.0167487 N. Using the Peltier effect of the semiconductor material, when direct current passes through a galvanic couple of two different semiconductor materials in series, heat can be absorbed and released at the corresponding side of the galvanic couple, thus achieving the purpose of cooling. This is a refrigeration technology that produces negative thermal resistance and has no moving parts and high reliability. The results of heat flow analysis are shown in Figs. 14 and 15.

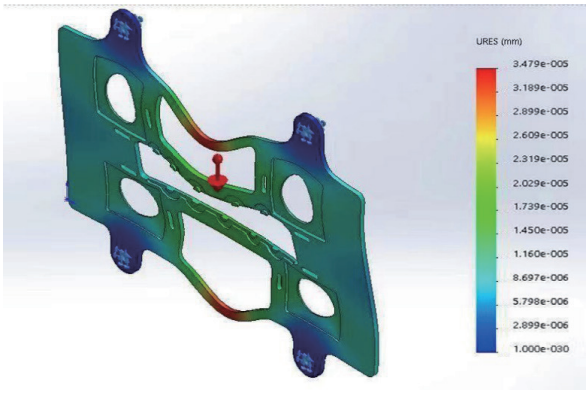

Fig. 12. (Color online) Displacement of front shield.

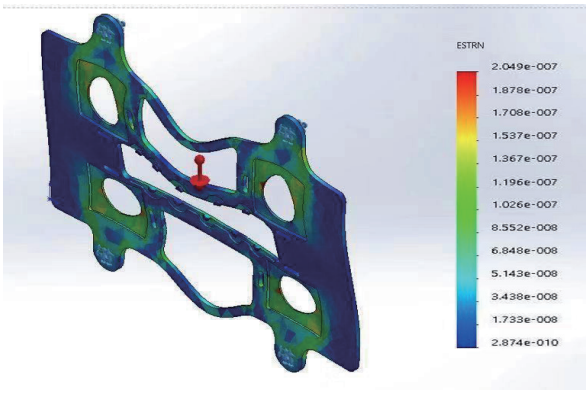

Fig. 13. (Color online) Strain of front shield.

Fig. 14. Heat flow of rear shield.

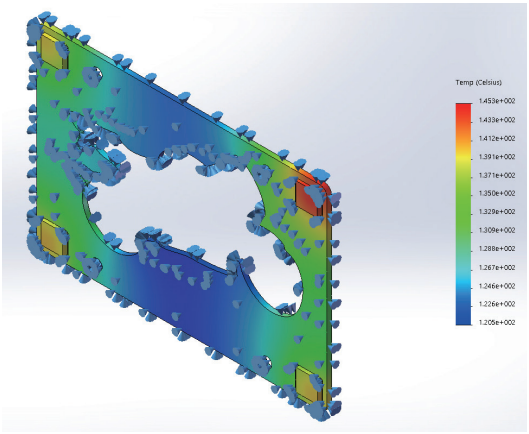

Fig. 15. (Color online) Heat flow of rear shield.

The products designed on the basis of the above themal finite element analysis and experiment are shown in Figs. 16–19. Figure 16 shows the self-designed water tank. It uses 6061 aluminum alloy, which has good plasticity and excellent corrosion resistance, no stress corrosion cracking tendency, excellent weldability, and good cold workability. The operation range is from 120.512 to 145.333 °C, where the maximum temperature is less than the melting point of aluminum of 660.37 °C. Thus, the requirements for the heat flow are met. The temperature difference is 24.821 °C, which also satisfies the requirement of the temperature difference for power generation. Figure 17 shows the temperature-measuring device and its circuit. The circuit is controlled by an Arduino chip. Figure 18 shows the results of the test using the app.

The Pt100 is connected with a Wheatstone bridge, an operational amplifier, and a Bluetooth module. The temperature change induces a voltage difference between the two ends of the bridge. The voltage is amplified by a factor of 4 through an operational amplifier and acts as the AD input of the Arduino chip. The current temperature value is calculated and sent to the computer via Bluetooth.

The main points of this study are summarized as follows:

1. Common vehicles driven by fuels (gasoline, diesel, and aviation oil) are equipped with water tanks, which are used to dissipate heat.
2. The thermal energy on a water tank is lost as waste heat and is not fully utilized.
3. In this research, a multifunctional cooling water tank that generates electric energy from thermal energy is designed. It also has anti-theft and power storage functions.
4. The production process is simple, fast, and cost-effective. Moreover, the cost can be reduced by mass production, and its prospects for commericalization are promising.
5. Resources from universities and industry can be integrated to jointly develop new technologies and products.

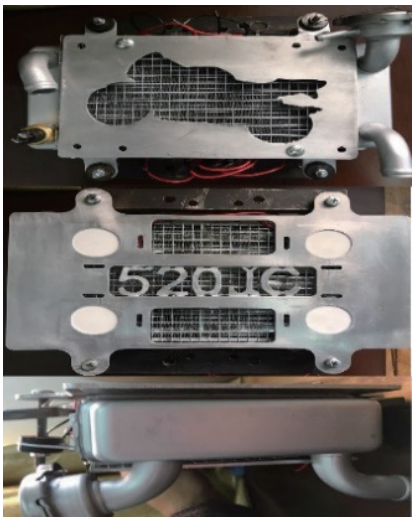

Fig. 16. (Color online) Designed water tank.

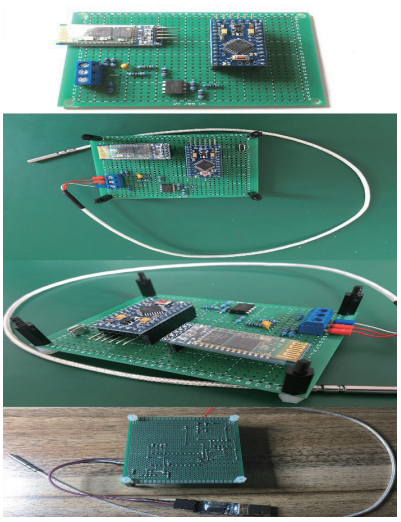

Fig. 17. (Color online) Temperature-measuring device.

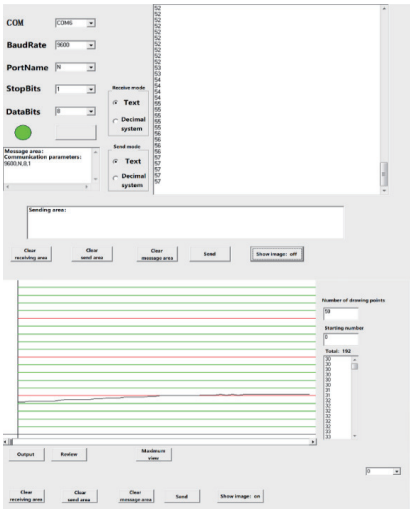

Fig. 18. (Color online) Results of computer test.

Fig. 19. (Color online) Schematic of the simulation vehicle.

4. Conclusions

This paper describes an innovative design that recycles thermal energy into electric energy for vehicles. In the proposed design, a shield is mounted on the outside of the water tank of a traditional heavy-duty locomotive to protect the water tank. Such a shield is installed with a detachable number plate as a spare locomotive number to prevent the loss of a number plate due to theft or other reasons. On the other hand, thermoelectric power generation chips are mounted at the four corners of the front and rear panels of the shield and use the heat from the water tank to generate electric energy. By employing the proposed design, energy can be recycled and reutilized to reduce environmental impact and conserve energy. Furthermore, the

research results of this paper can be used for talent cultivation and research and development. In summary, it provides a foundation for integrating a wide range of resources for vocational education in practical technology.

References

1 T. H. Hoang, A. T. Hoang, and V. S. Vladimirovich: Energy Sources, Part A (2019). https://doi.org/10.1080/15567036.2019.1630035
2 Z. H. Dughaish: Physica B **322** (2002) 205.
3 K. Yavuz, O. A. Ekber, and A. Tahsin: J. Solar Energy Eng. **140** (2018) 6.
4 E. Michael, B. Klas, R. Ulrich, B. Tobias, G. Gerd, D. S. Melina, and A. Dag: Microelectron. Reliab. **55** (2015) 722.
5 Y. Apertet and H. Ouerdane: Energy Convers. Manage. **149** (2017) 564.
6 S. Saima, J. Slavisa, and P. Philippe: Energies **10** (2017) 3.
7 G. Andreas and I. S. Beloborodov: Phys. Rev. B **79** (2009) 23.
8 T. Khaled, Z. Youtong, and M. X. Long: Energies **11** (2018) 576.
9 Q. Rui, G. Y. Liu, C. G. Wang, and Z. Wei: Yadong: Coatings **8** (2018) 45.
10 S. Gary, Y. Kazuaki, and B. C. Avram: IEEE Trans. Adv. Pack. **31** (2008) 429.